Optical Phase Conjugation for Ultra Long-Haul Phase-Shift-Keyed Transmission

S. L. Jansen, *Student Member, IEEE*, D. van den Borne, *Student Member, IEEE*, B. Spinnler, S. Calabrò, H. Suche, P. M. Krummrich, *Member, IEEE*, W. Sohler, G.-D. Khoe, *Fellow, IEEE*, and H. de Waardt

***Abstract*—Nonlinear phase noise (Gordon–Mollenauer phase noise) can limit the transmission distance for phase-shift-keyed modulation formats. In this paper, the compensation of nonlinear phase noise by a midlink optical phase conjugation (OPC) is studied. A proof-of-principle experiment is presented showing an over 4-dB improvement in Q factor when OPC is employed in a differential phase-shift-keying (DPSK) system. Also, an ultra long-haul OPC-based differential quadrature phase-shift-keying (DQPSK) transmission experiment is studied to show the impact of self-phase modulation (SPM)-induced impairments, including nonlinear phase noise, in a transmission line. OPC results in a 44% increase in transmission distance when compared to a "conventional" transmission system using dispersion compensating fiber (DCF) for chromatic dispersion compensation.**

***Index Terms*—Alternative modulation formats, differential phase-shift keying (DPSK), differential quadrature phase-shift keying (DQPSK), dispersion compensation, fiber optics communications, nonlinear phase noise, periodically poled lithium niobate (PPLN), phase conjugation, phase-shift keying, spectral inversion.**

I. Introduction

RECENTLY, a strong interest has been shown in phase-shift-keyed modulation formats for long-haul transmission [1]. The most promising phase-shift-keyed modulation formats are differential phase-shift keying (DPSK) and differential quadrature phase-shift keying (DQPSK). The main advantages of DPSK over amplitude shift keying (ASK) are that DPSK has, in combination with balanced detection, a 3-dB higher sensitivity and is more robust to narrowband optical filtering [2]. The advantages of DQPSK are favorable spectral width and high tolerances for chromatic and polarization-mode dispersion at the same bit rate as binary modulation [3], [4]. However, phase-shift-keyed transmission suffers from increased impact of nonlinear-phase-noise (Gordon–Mollenauer phase noise) degradation [5], [6].

Manuscript received June 30, 2005; revised November 17, 2005.

S. L. Jansen, D. van den Borne, G.-D. Khoe, and H. de Waardt are with the Communication Technology Basic Research and Applications (COBRA) Institute, University of Technology, Eindhoven 5612 AZ, The Netherlands (e-mail: s.l.jansen@tue.nl; dirk@vandenborne.com; g.d.khoe@tue.nl; h.d.waardt@tue.nl).

B. Spinnler is with Siemens Aktiengesellschaft (AG), Corporate Technology, Information and Communications, Munich D-81730, Germany (e-mail: bernhard.spinnler@siemens.com).

S. Calabrò and P. M. Krummrich are with Siemens AG, Communications (COM), Fixed Networks, Munich D-81359, Germany (e-mail: stefano.calabro@siemens.com; peter.krummrich@siemens.com).

H. Suche and W. Sohler are with the Universität Paderborn, Department Physik, Paderborn D-33098, Germany (e-mail: suche@physik.upb.de; sohler@physik.uni-paderborn.de).

Digital Object Identifier 10.1109/JLT.2005.862481

Several optical compensation schemes have been proposed to compensate for nonlinear phase noise. However, only few successful experiments have so far been reported—post-transmission nonlinear phase-shift compensation (NPSC) [7], semiconductor optical amplifier (SOA)-based regenerative amplification [8], and optical phase conjugation (OPC) [9], [10].

OPC, which is a promising method to compensate for nonlinear phase noise, is a technique where the spectrum of the data signal is inverted in the transmission link (typically in the middle) [11]–[18]. Impairments experienced in the first part of the link are then cancelled out with the impairments in the second part of the transmission link. It has been experimentally shown that OPC can compensate for chromatic dispersion [11]–[15], self-phase modulation (SPM), [16] and also intra-channel nonlinear impairments [17]–[19]. The key advantages of OPC are that simultaneous processing of multiple channels is possible [20] and that an OPC is transparent to modulation format and data rate [21].

In this paper, the compensation of SPM-induced nonlinear phase noise by OPC is discussed, enabling 21.4-Gb/s DQPSK transmission over $> 10\,000$ km. In Section II, we show that the OPC can be employed to compensate for SPM-induced nonlinear phase noise. In this proof-of-principle experiment, the effect of nonlinear phase noise is emphasized by using a high fiber input power and by artificially reducing the optical signal-to-noise ratio (OSNR) before transmission. We show that at low transmitted OSNRs, where the effect of the phase noise is strongest, over 4 dB of improvement in Q factor can be realized through the use of OPC.

Section III describes an ultra long-haul 21.4-Gb/s DQPSK transmission experiment. In this experiment, the performance of OPC for compensation of chromatic dispersion and nonlinear impairments is compared to conventional dispersion compensating fiber (DCF)-aided transmission. We show that the performance of the DCF-based scheme is severely impaired by SPM-induced impairments such as nonlinear phase noise, whereas the performance of the OPC is virtually unaffected.

II. Compensation of Nonlinear Phase Noise: Proof of Principle

In this section, a proof-of-principle experiment is described to show that OPC can effectively compensate for impairments due to nonlinear phase noise. Initial results of this proof-of-principle experiment are reported in [9]. In these experiments, the inversion of the sign of the effective chromatic

0733-8724/$20.00 © 2006 IEEE

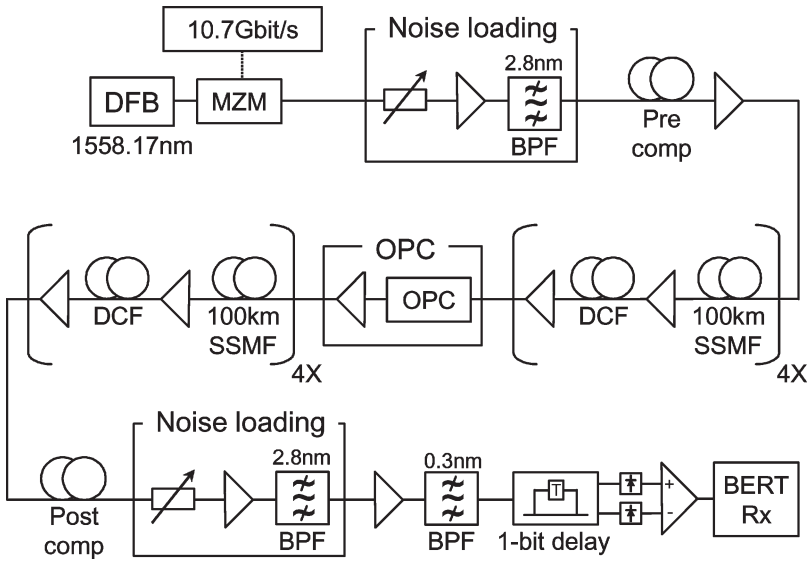

Fig. 1. Experimental DPSK transmission setup with and without OPC.

dispersion due to OPC is not cancelled. Improved results where the effective dispersion map is maintained are reported in [10].

A. Nonlinear-Phase-Noise Impairment on DPSK Transmission

The experimental setup is depicted in Fig. 1. This proof-of-principle experiment was single channel in order to assess only SPM-induced nonlinear phase noise. A nonreturn-to-zero (NRZ)-DPSK signal is generated at 1558.2 nm by a distributed feedback (DFB) laser and a Mach–Zehnder modulator (MZM) in a push-pull configuration. The bit rate is 10.7 Gb/s, and the length of the pseudorandom bit sequence used is $2^{31}-1$. Before transmission, a noise generation scheme consisting of an attenuator, an optical amplifier, and a bandpass filter (BPF) is inserted, enabling setting the OSNR of the data signal at the system input. Also, the signal is precompensated by a DCF with -510 ps/nm.

The transmission line consists of eight spans of 100-km standard single-mode fiber (SSMF). After each span, a DCF module is used to compensate for the chromatic dispersion. The average undercompensation per span is 55 ps/nm. Erbium-doped fiber amplifiers (EDFAs) are used between each SSMF and DCF module to compensate for the fiber loss. In the 800-km long transmission line, the effect of nonlinear phase noise will not be clearly present for optimized transmission parameters. Nonlinear phase noise is an interaction between an amplified spontaneous emission (ASE) and an SPM. Hence, we enhance the effect of nonlinear phase noise by artificially reducing the OSNR at the transmitter (to increase ASE noise) and by using high input powers into the SSMF (to enhance SPM). The input powers into the SSMF and DCF are 11.5 and 1.5 dBm, respectively. The loss of the SSMF spans varied between 21 and 24 dB, and the loss of the DCF modules varied between 10 and 13 dB.

After transmission, the postcompensation is optimized to achieve the minimum bit error rate (BER). Throughout this paper, Q factors in decibels will be reported as computed by (1).

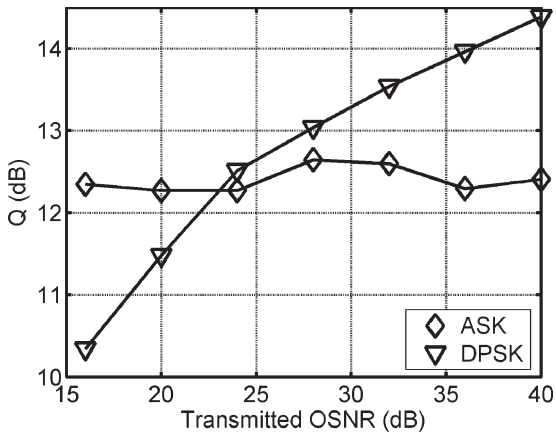

Fig. 2. Q factor at 12-dB received OSNR as a function of the transmitted OSNR for the DPSK and ASK modulation formats (res. bw. $= 0.1$ nm).

$$\mathrm{Q} = 20\log\left(\sqrt{2}\times erfcinv(2\times \mathrm{BER})\right). \tag{1}$$

At the receiver, the OSNR is kept constant at 12 dB using an attenuator, an EDFA, and a 2.8-nm BPF. Subsequently, a 0.3-nm BPF removes the out-of-band ASE. The DPSK detector consists of a Mach–Zehnder delay interferometer (MZDI) with a 1-bit delay (93.5 ps), a balanced receiver, and a 10.7-Gb/s BER tester.

Fig. 2 shows the Q factor after the 800-km transmission as a function of the transmitted OSNR for DPSK and ASK. The OSNR at the receiver is kept constant at 12 dB by noise loading at the system output. At a high transmitted OSNR (40 dB), the DPSK modulation format performs over 2-dB better in Q factor than the ASK modulation format. Similar to the results reported in [6], the performance of the DPSK modulation format is severely affected by nonlinear phase noise when the OSNR of the transmitter is reduced, whereas for the ASK modulation format, the performance is unaffected. As a result, when the

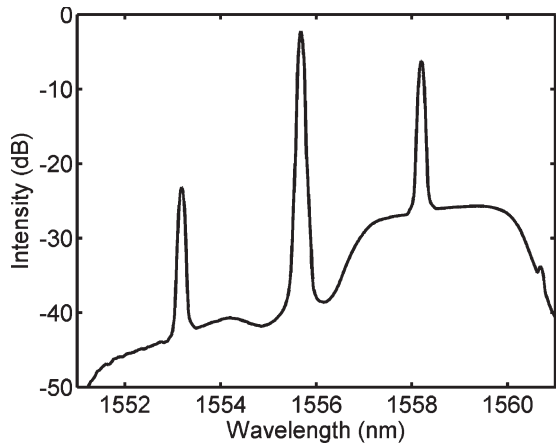

Fig. 3. Optical spectrum after the SOA (res. bw. = 0.1 nm).

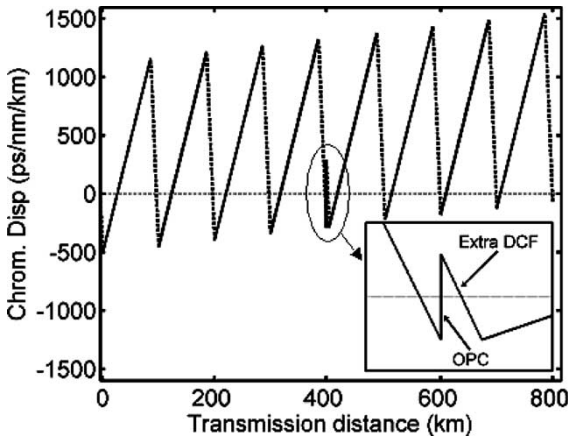

Fig. 4. Chromatic dispersion as a function of the transmission distance for the link with OPC.

transmitted OSNR is reduced to 16 dB, the performance of the DPSK modulation format is about 2-dB worse than the performance of the ASK modulation format.

B. OPC for Nonlinear-Phase-Noise Compensation

In order to study the effect of OPC on the impairments due to nonlinear phase noise, a phase conjugator is added in the middle of the 800-km transmission line.

OPC can be used to compensate for the chromatic dispersion. In such an application, the inline DCF is removed from the transmission line resulting in a nonperiodic dispersion map. However, in this proof-of-principle experiment, the effect of a nonperiodic dispersion map on the nonlinear-phase-noise penalty is excluded. For this reason, the same effective dispersion map is used in this experiment for the DCF-aided and the OPC-aided transmission systems.

OPC of the data signal is realized by a four-wave mixing (FWM) in an SOA. Fig. 3 shows the experimental setup of the SOA-based OPC subsystem. The data is combined with the amplified output of a DFB pump laser and fed into a 2-mm long SOA. Inside the SOA, the pump signal at 1555.7 nm and the data signal at 1558.2 nm generate an FWM product at 1553.3 nm. Fig. 4 depicts the optical spectrum after the SOA.

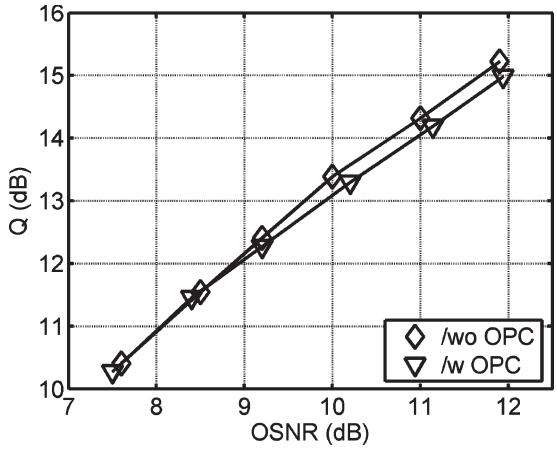

Fig. 5. Back-to-back Q factor as a function of the OSNR with and without OPC (res. bw. = 0.1 nm).

In this plot, the three signals—an incoming data signal at 1558.2 nm, a continuous-wave (CW) pump signal at 1555.7 nm, and the FWM product at 1553.3 nm—can be identified.

The injection current of the SOA is set to 730 mA, and the input optical powers into the SOA are 11 and -1 dBm for the control and the data signals, respectively. The saturation power of the SOA is 8 dBm. After conversion, the pump is removed by a fiber Bragg grating (FBG). An isolator prevents the light reflected by the FBG from propagating back into the SOA. Finally, the original data signal is removed using an 8-nm BPF.

The phase-conjugated signal has the inverted signal spectrum from the incoming data signal. Through this process, the sign of the effective cumulative chromatic dispersion is also inverted. Similar to [22], the same cumulative dispersion as in the non-OPC configuration is obtained by using a DCF module after OPC to shift the effective accumulated chromatic dispersion to the value it has before OPC. The chromatic dispersion as a function of the transmission distance for the link with OPC is depicted in Fig. 4.

The conversion efficiency, defined as the difference in optical power levels between the input and the converted output data signal, is -16.4 dB. Fig. 5 depicts the back-to-back Q factor as a function of the OSNR with and without OPC. The measured OSNR penalty due to OPC is ~ 0.2 dB. This is a good indication that the contribution of the FWM conversion processes and the SOA to nonlinear impairments is small and can be neglected.

The Q factor as a function of the transmitted OSNR for the transmission system with and without OPC is plotted in Fig. 6. At a high transmitted OSNR (40 dB), where the effect of nonlinear phase noise is low, the OPC-based configuration shows a 1-dB improvement in Q factor compared to the DCF-based configuration. The simulations discussed in Section II-C will show that the improvement in Q factor at a high transmitted OSNR results from a compensation of the SPM through OPC. At low transmitted OSNR (16 dB), where the influence of nonlinear phase noise is the largest, the Q factor of the system without OPC decreases by almost 4 dB, whereas the Q factor of the link with the OPC decreases by less than 1 dB. Thereby, at

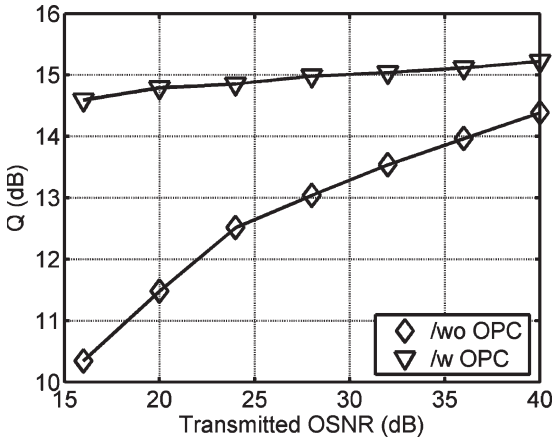

Fig. 6. Experimental result: Q factor as a function of the transmitted OSNR for DPSK transmission with and without OPC (res. bw. $= 0.1$ nm).

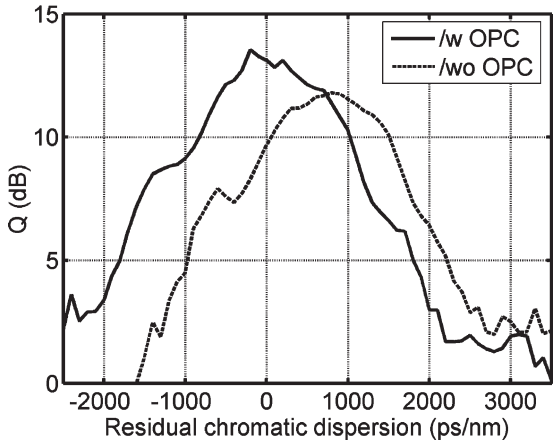

Fig. 7. Simulation: Q factor as a function of the residual dispersion with and without OPC.

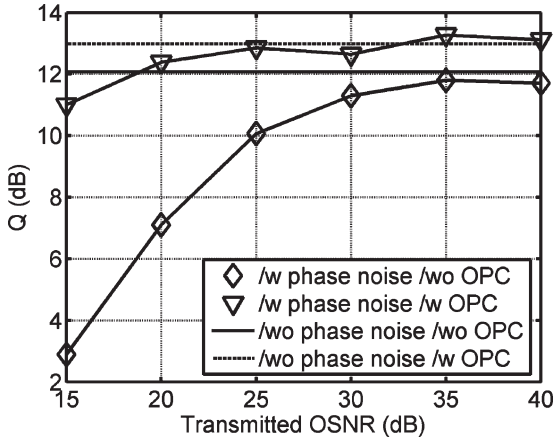

Fig. 8. Simulation: Q factor as a function of the transmitted OSNR at 9-dB received OSNR, with and without OPC.

a low transmitted OSNR, over 4 dB of improvement in Q factor is obtained for the OPC-based configuration compared to the system without OPC.

C. Verification Through Simulations

The experimental results presented in Section II-B are verified by simulations [23]. In these simulations, the propagation of the signal is simulated using a linear convolution (asymmetric) split-step Fourier algorithm. The noise figure of the inline amplifiers is 4 dB. ASE noise is added at the transmitter and at every amplifier along the line, and the interaction of ASE and the signal due to the SPM is taken into account. Monte Carlo simulations are used to estimate the Q factor. Fragments of a pseudorandom binary sequence (PRBS) with a length of $2^{32}-1$ are used in the simulation. The maximum length of the bits simulated per point is 2 000 000. In order to reduce the simulation time, the bit sequence is divided into smaller blocks that can be processed by fast Fourier transform (FFT) methods. The number of points for the FFT is 8192, and the dependencies between the blocks are taken into account by the overlap-add method [24]. Additionally, the simulation for a certain point is stopped when 100 errors occurred.

The simulation bandwidth is 16 samples per bit, and the step size was chosen so that the maximum nonlinear phase shift is 0.1°. It was verified that a smaller step size does not change the results. The reliability of the results of the Monte Carlo simulations depends on the number of transmitted bits "N" and the number of errors "n" and can be estimated by means of confidence intervals [24], e.g., for $N = 10^6$ and $n = 10^2$, the probability that $8 \times 10^{-5} < \text{BER} < 1.2 \times 10^{-4}$ is 99%. The dispersion map, the input powers, and the span count are equal to those of the experimental setup. The decision threshold for the DPSK signal is fixed to 0.

For the simulation, an ideal phase conjugation is assumed; since in the experimental setup, a power penalty of only less than 0.2 dB is measured for OPC. The amount of postcompensation is optimized for operation with and without OPC individually at a high transmitted OSNR. Fig. 7 depicts Q factor as a function of the residual chromatic dispersion at a high transmitted OSNR. With OPC, most SPM is compensated for through-phase conjugation; hence, the accumulated dispersion is optimal around 0 ps/nm. Without OPC, the positive residual dispersion is optimal after transmission since the dispersion partly compensates the SPM. The residual dispersions used in the simulations are -202 ps/nm and 798 ps/nm for the system with and without OPC, respectively.

Fig. 8 depicts the Q factor with and without OPC with optimized postcompensation. The receiver OSNR is kept constant at 9 dB. The receiver OSNR in the simulations is set lower than in the experiments, since the used Monte Carlo approach restricts the maximum Q factor that can be simulated with reasonable computation effort. We also carried out simulations with and without OPC, where the effect of nonlinear phase noise is switched off. In these simulations, noise is computed analytically and added at the receiver. The transmitted OSNR in these simulations does not influence the Q factor after transmission and are represented in Fig. 8 as horizontal lines.

Comparing the simulation (Fig. 8) and the experimental (Fig. 6) results, a good agreement can be seen. In both the simulation and the experiment, a $\sim$ 1-dB Q-factor difference is present at high transmitted OSNR, whereas at low transmitted OSNR, the difference in Q factors increases to over 4 dB due to the compensation of nonlinear phase noise. When the effect of nonlinear phase noise is neglected and the noise is

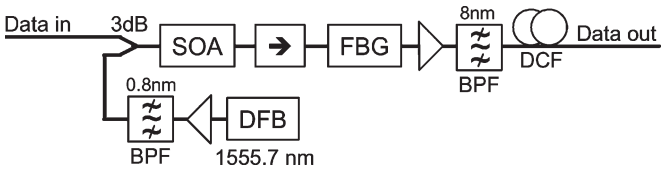

Fig. 9. Layout of the SOA-based OPC subsystem.

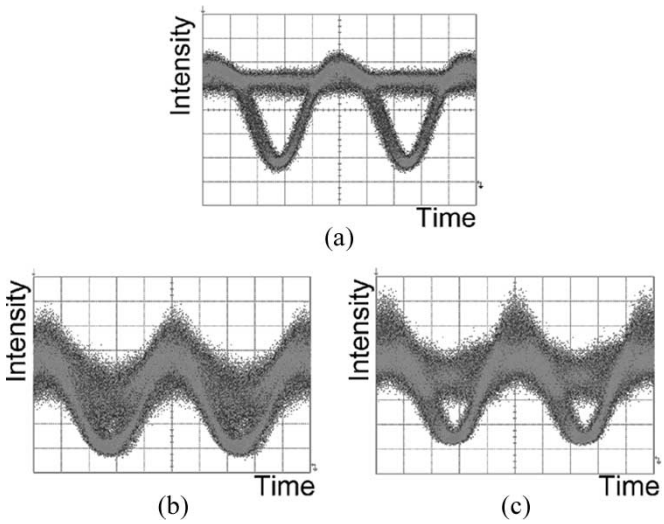

Fig. 10. Phase eye diagrams of the NRZ-DPSK signal (a) back-to-back, (b) after transmission at high transmitted OSNR (40 dB) without OPC, and (c) with OPC.

computed analytically, a $\sim$ 1-dB improvement in Q factor is still present. Hence, we conclude that the improvement at a high transmitted OSNR is due to the SPM compensation in the OPC configuration.

The compensation of SPM is also evident in the experimental phase eye diagrams. The "phase eye diagram" refers to the eye diagram before the 1-bit delay (see Fig. 9). Fig. 10(a) shows the back-to-back phase eye diagram of the NRZ-DPSK signal. Fig. 10(b) and (c) shows the phase eye diagrams after transmission at a high transmitted OSNR with and without OPC, respectively. It can be seen that the phase eye diagram is less distorted when OPC is employed.

D. OPC Placement

In order to test the dependence of the Q factor on the location of the OPC-unit within the link, the unit is placed in several locations and the Q factor is measured. The Q factor after the 800-km transmission link for the highest (40 dB) and the lowest (16 dB) transmitted OSNRs is plotted in Fig. 11. The two lines at a Q factor of 10.4 dB and a Q factor of 14.5 dB represent the performance of the system without OPC at the 16-dB and the 40-dB transmitted OSNR, respectively. The OSNR at the receiver is kept constant at 12 dB.

The system with OPC performs best for both high and low transmitted OSNR, when the device is placed in the middle of the link. The least effective measured location of the OPC is after the first ($X = 1$, $Y = 7$) span or before the last ($X = 7$, $Y = 1$) span. The performance at these places is comparable

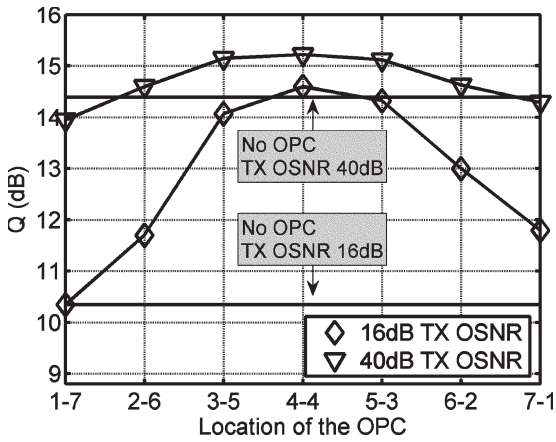

Fig. 11. Q factor as a function of the location of the OPC $(X-Y)$, where $X =$ number of spans before OPC and $Y =$ number of spans after OPC.

to the performance of the transmission link without OPC. Through OPC, a signal is regenerated indirectly—the phase of the signal is conjugated; hence, the signal distortions are reverted along the rest of the transmission line. When the OPC-unit is placed too early in the link, no distortions occurred yet; hence, the cancellation effect is small. When the OPC-unit is placed near the end of the transmission link, the signal distortions cannot be totally reverted in the rest of the transmission line. This reduces the cancellation effect as well. Additionally, the OSNR is reduced in the OPC-unit due to the noise of the SOA, which causes impairments due to nonlinear phase noise in the transmission path after OPC.

In order to show the effect of nonlinear phase noise in the 800-km proof-of-principle experiment, noise is added at the transmitter. In a real-world transmission system, noise accumulates along the line and is not artificially introduced. However, this also affects the optimum placement of the OPC-unit in a transmission line to optimally compensate for the impairments through nonlinear phase noise. It has been shown that the optimum placement for the OPC-unit is at 66% in a real-world transmission line [25], as opposed to 50%, as found for the proof-of-principle experiment. However, as we have shown in Fig. 11, the compensation of nonlinear phase noise through OPC is highly tolerant to the placement of the OPC. In the next section, we show that in long-haul transmission without noise loading at the transmitter, midlink OPC (50% placement) is able to compensate for the detrimental impact of SPM-induced nonlinear impairments, including nonlinear phase noise. This makes it possible to combine both nonlinear-phase-noise compensation and chromatic dispersion compensation, thereby utilizing both interesting aspects of OPC.

III. Ultra Long-Haul DQPSK Transmission

Section III describes an ultra long-haul DQPSK transmission experiment comparing the performance of DCF-aided and OPC-aided transmissions. Since in this experiment OPC is not only used for the compensation of nonlinear impairments but also for chromatic dispersion compensation, the OPC-unit is placed in the middle of the transmission link.

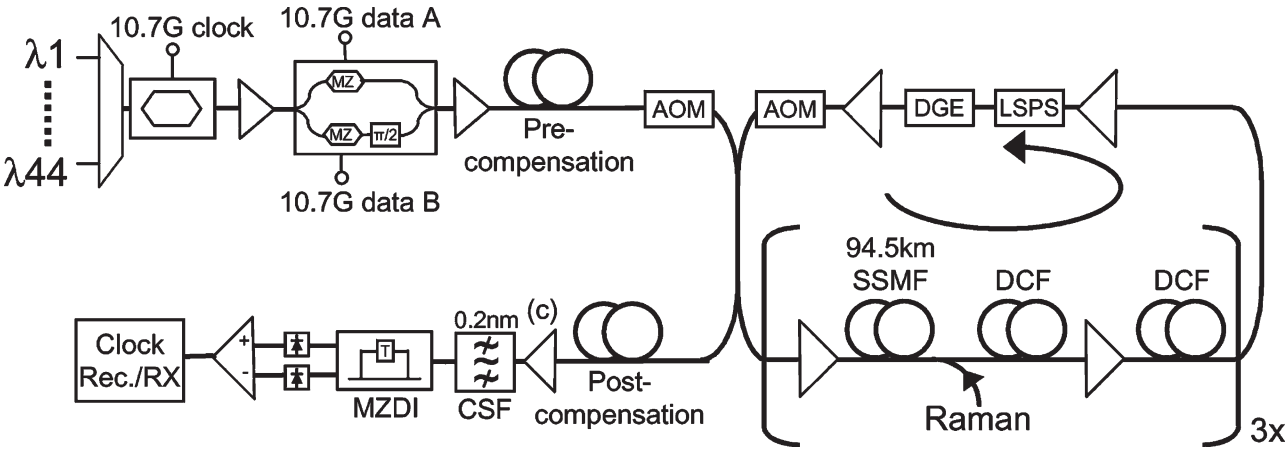

Fig. 12. Experimental setup of the DCF-aided transmission link.

A. DCF-Aided DQPSK Transmission

The experimental setup of the DCF-aided recirculating loop is depicted in Fig. 12. At the transmitter, 44 CW signals on a 50-GHz grid are generated in the C band by DFB lasers and multiplexed by using an arrayed waveguide grating (AWG). Subsequently, a modulator cascade consisting of two external $LiNbO_3$ MZMs is used to generate return-to-zero (RZ) DQPSK. The first modulator is driven with a 10.7-GHz clock signal, carving a pulse with a 50% duty cycle. The second modulator is an integrated DQPSK modulator with two parallel MZMs within a super Mach–Zehnder structure. The relative phase shift between the two parallel modulators is $\pi/2$. Two 10.7-Gb/s data streams (one inverted: data A, one noninverted: data B) with a relative delay of 5 bits for decorrelation of the bit sequences are used for modulation of the 21.4-Gb/s DQPSK signal. The length of the PRBS used is $2^{15}-1$. In this experiment, no longer PRBS length can be used without precoding since the DQPSK modulation format requires the BER test set (BERT) to be programmed.

The transmission line consists of three 94.5-km spans of SSMF with an average span loss of 21.5 dB and a chromatic dispersion of $\sim$ 16 ps/nm/km. The loss of the SSMF spans is compensated by using a hybrid Raman/EDFA structure for signal amplification. The average ON/OFF Raman gain of the backward pumped Raman pumps is $\sim$ 11 dB. After each span, a DCF module is used to compensate for the chromatic dispersion. To balance the DCF insertion loss, 20% of the DCF is placed between the Raman pump and the first stage of the inline amplifier. A loop-synchronous polarization scrambler (LSPS) is used to reduce the statistical correlation of loop-induced polarization effects. Power equalization of the dense wavelength division multiplexing (DWDM) channels is provided by a channel-based dynamic gain equalizer (DGE) with a bandwidth of 0.3 nm. Hence, spectral filtering of the signals occurs with every recirculation. After transmission, the dispersion is optimized on a per-channel basis. A 0.2-nm channel-selection filter (CSF) is used to select the desired channel. After a 1-bit (94 ps) MZDI and a balanced detector, the clock is recovered and the performance of the signal is evaluated using a BERT programmed for the expected output sequence.

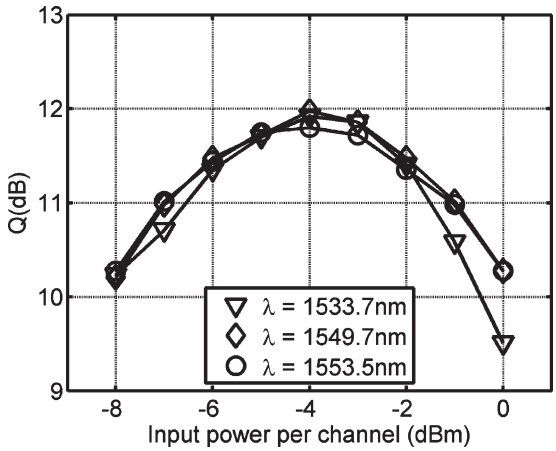

Fig. 13. Q factor as a function of the input power per channel.

In order to optimize the performance of the DCF-based transmission system, the optical input power into the SSMF, the inline dispersion map, and the precompensation is optimized at a 4500-km transmission distance. For this optimization, the Q-factor performance is measured of three typical channels, namely 1533.9, 1549.7, and 1553.7 nm. The Q factor as a function of the input power per channel is depicted in Fig. 13. The inline undercompensation in the input power variation experiment is set to $\sim$ 80 ps/nm/span, and the precompensation is fixed to -850 ps/nm.

When a low input power into the SSMF is used (-8 dBm per channel), the transmission is OSNR limited. At a high input power, the system is limited by nonlinear impairments. An optimum input power of -4 dBm/channel is used in the transmission experiment. Fig. 14 shows the Q factor as a function of the inline undercompensation per span. The input power is set to -4 dBm/channel, and a precompensation of -850 ps/nm is used.

At a low inline undercompensation, the influence of cross-phase modulation (XPM) and XPM-induced nonlinear phase noise becomes more severe due to insufficient walk-off between the channels [26]. No decrease in Q factor is detected up to an undercompensation of 110 ps/nm/span. A large undercompensation is impractical for ultra long-haul transmission, since

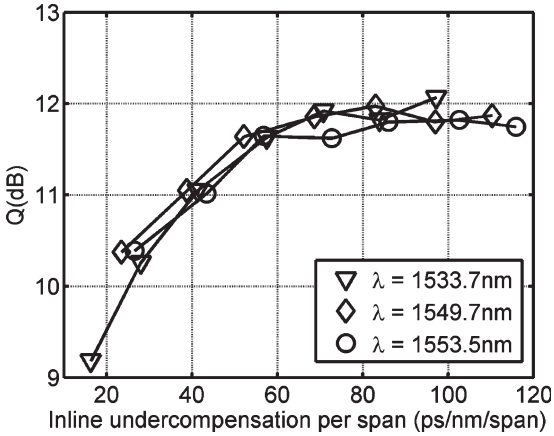

Fig. 14. Q factor as a function of the inline undercompensation per span.

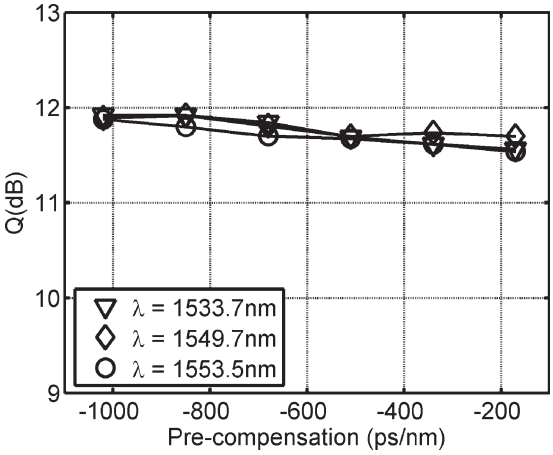

Fig. 15. Q factor as a function of the precompensation.

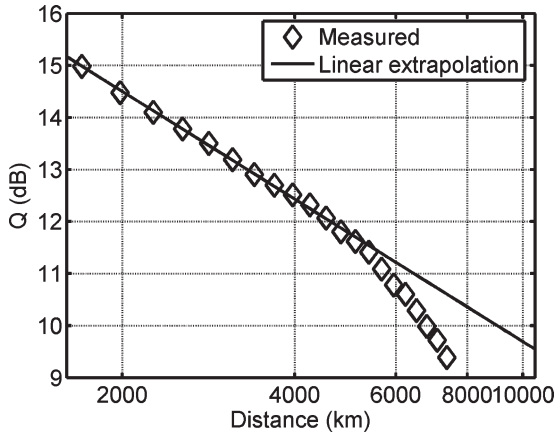

Fig. 16. DCF-aided transmission: Q factor of a typical channel as a function of transmission distance.

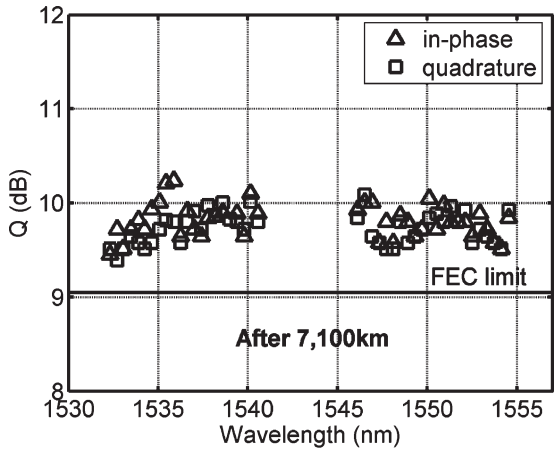

Fig. 17. In-phase and quadrature Q factors for the DCF-based configuration.

huge amounts of postcompensation are then required at the receiver. Considering this tradeoff, an undercompensation of around 80 ps/nm/span is chosen.

In Fig. 15, the Q factor is plotted as a function of the precompensation. In this experiment, the input power is set to -4 dBm/channel and the inline undercompensation is fixed to 80 ps/nm/span. From this plot, we can conclude that the amount of precompensation does not have a strong influence on the performance of the DQPSK transmission. The precompensation used in the transmission experiment is -850 ps/nm. Using these optimized parameters, the Q factor of a typical channel (in phase, 1550.7 nm) is assessed as a function of the transmission distance as plotted in Fig. 16.

At shorter distances, the Q factor shows a linear decrease with an exponential increase in the transmission distance. After a 5000-km transmission, the Q factor deviates from the linear decrease. For the RZ-DQPSK modulation format, it has been shown that single-channel impairments are dominant over multichannel impairments [3]. Hence, we conjecture that the degradation in the Q factor of the DCF-aided transmission results from SPM-induced impairments such as nonlinear phase noise as previously observed in [27].

The Q factors of all 44 wavelengths after 7100 km (25 circulations through the recirculating loop) are shown in Fig. 17. Both the in-phase and quadrature channels are depicted.

All Q factors are above a forward error correction (FEC) threshold of a concatenated code with a 7% redundancy, for which a Q factor of 9 dB corresponds to a performance after FEC with a BER of $< 1 \times 10^{-12}$ [28].

B. OPC-Aided DQPSK Transmission

The experimental setup of the OPC-aided configuration is depicted in Fig. 18. In the OPC-based configuration, the inline DCF modules for chromatic dispersion compensation are removed, and an OPC-unit is inserted in the middle of the transmission link for compensation of dispersion and nonlinear impairments [29]. Apart from that, the components (transmitter, receiver, SSMF, amplifiers, etc.) are the same as in the DCF-based configuration discussed in the previous section.

The Raman gain in the OPC experiment is the same as in the DCF-based experiment. It has been shown in [17] that the compensation of the Kerr effect is optimal when a power-symmetric transmission link is realized. The average net Raman gain in this experiment is -10.3 dB. This is significantly below the gain required for power symmetry. The input power per channel into the SSMF is -2.9 dBm (13.5-dBm total input power). In this wavelength division multiplexing (WDM) OPC transmission experiment, simultaneous conversion of multiple WDM channels is required. Hence, instead of the FWM-based

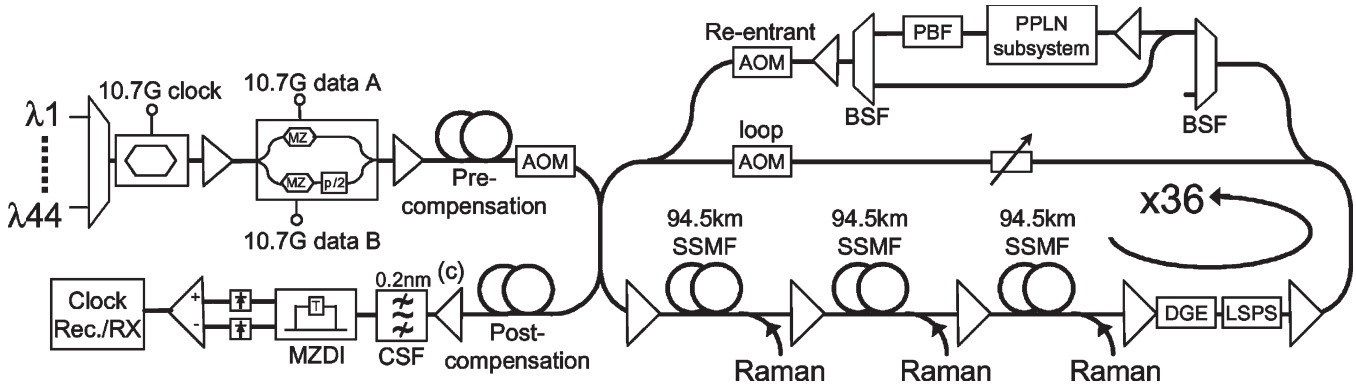

Fig. 18. Experimental setup of the OPC-aided transmission link.

OPC we described in Section II, a periodically poled lithium niobate (PPLN) is used for OPC. The advantages of the PPLN for OPC are that the PPLN is immune to χ^3-based optical nonlinear interactions such as SPM and XPM, converts up to 70 nm with a single device, and has low crosstalk and low additive noise [30], [31].

The signals are optically phase conjugated in the middle of the transmission link. In the reentrant recirculating loop structure, this is realized after half the recirculations ($18\times$) by opening the loop acousto-optic modulator (AOM) and closing the reentrant AOM for one recirculation. Hereby, the signals are fed through the PPLN subsystem. In this subsystem, the 22 channels from 1532.3 to 1540.6 nm that were used to balance the signal in the amplifiers are removed using a band selection filter (BSF). Subsequently, the remaining 22 channels from 1546.1 to 1554.5 nm are phase conjugated in the PPLN subsystem. At the output of the PPLN subsystem, the wavelengths of the channels range from 1532.3 to 1540.6 nm. Finally, the input channels of the PPLN subsystem (ranging from 1546.1 to 1554.5 nm) are recombined with the spectrally inverted channels to balance the signal propagating through another 18 circulations in the recirculating loop.

The phase conjugation inside the PPLN waveguide is realized by two quasi-phase-matched χ^2 processes [30], [31]. A second harmonic from a pump is generated through a second-harmonic generation. Simultaneously, the second harmonic interacts with the incoming data signal through difference frequency mixing. Quasi-phase matching is realized inside the PPLN by reversing the sign of the nonlinear susceptibility every 16.3 μm. At the output of the PPLN, the phase-conjugated signals are present mirrored with respect to the pump. Fig. 19 depicts the optical spectrum (res. bw. $= 0.01$ nm) after the PPLN subsystem.

Similar to the DCF-aided transmission experiment, an LSPS is used to reduce the statistical correlation of loop-induced polarization effects. Hence, at the input of the PPLN subsystem, the channel polarizations are randomized by the transmission fiber and the polarization independence for the PPLN is required. A polarization-independent PPLN subsystem is realized by using both directions of propagation in a single PPLN [32].

The layout of the polarization-independent PPLN subsystem is depicted in Fig. 20. A polarization beam splitter (PBS) splits the incoming signal into transverse electric (TE) and

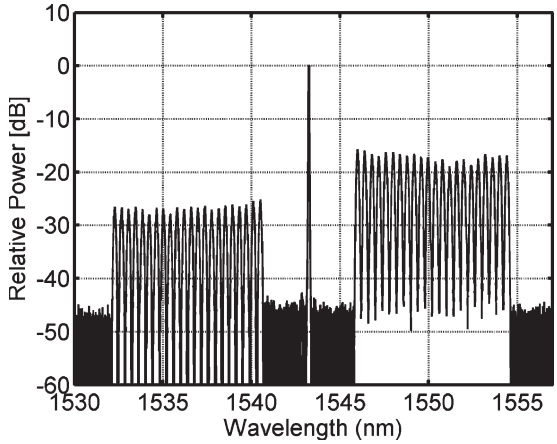

Fig. 19. Optical spectrum at the output of the OPC subsystem after 18 circulations in the loop (res. bw. $= 0.01$ nm).

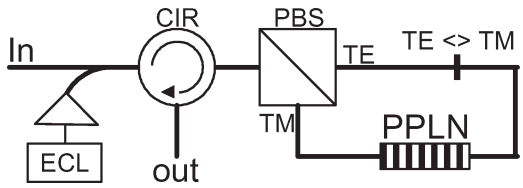

Fig. 20. Layout of the polarization-independent PPLN subsystem.

transverse magnetic (TM) modes. The TM mode is phase conjugated in the PPLN and subsequently rotated to the TE mode by a 90° splice. The TE mode is first converted from the TE mode to the TM mode and then phase conjugated. Both counterpropagating modes are recombined at the PBS to effectively create polarization-independent phase conjugation. The measured polarization-dependent loss of the PPLN subsystem is less than 0.4 dB. A CW pump signal is generated at 1543.4 nm using an external cavity laser (ECL) and amplified to 388 mW. In order to pump the PPLN in both directions, the pump is split in a 50%–50% ratio at the PBS. The power of the signal is approximately 10 mW per channel at the PBS. The conversion efficiency of the PPLN with these powers is -9.2 dB. The PPLN waveguide used for OPC operates at 202.3 °C in order to reduce the photorefractive effect.

Fig. 21 shows the measured Q factor of a typical channel (in phase, 1535.1 nm) as a function of the transmission distance.

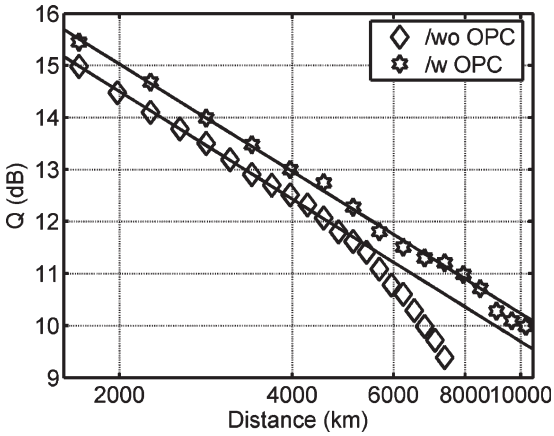

Fig. 21. Q factor of a typical channel as a function of transmission distance, with and without OPC.

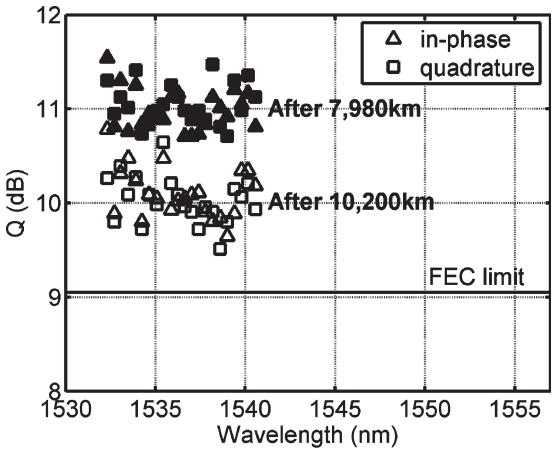

Fig. 22. In-phase and quadrature Q factors for the midlink OPC-based configuration.

As a reference, the typical channel (in phase, 1550.7 nm) of the DCF-aided transmission experiment is also depicted (same curve as in Fig. 16).

In the OPC-based configuration, the Q factor is about 0.5-dB higher than that of the DCF-based transmission system. After 5000 km, where the DCF-aided transmission is strongly impaired by nonlinear effects, the performance of the OPC-aided transmission is virtually unaffected.

Fig. 22 shows the Q factors for the OPC-aided transmission after 7980 km (28 circulations through the recirculating loop) and after 10 200 km (36 circulations through the recirculating loop). Both the in-phase and quadrature channels are depicted. Note that the Q factors are evaluated for the 22 phase-conjugated channels. A second OPC-unit would be required to conjugate and to enable measuring the other 22 channels. The worst Q factors are 10.7 and 9.5 dB after the 7940-km and the 10 200-km transmission, respectively. Both in-phase and quadrature components show similar performance. For the 7940-km transmission experiment, a 1.5-dB margin is measured with respect to the FEC threshold. When the transmission distance is increased to 10 200 km, the measured Q factors of all channels are still well above the FEC limit. In the DCF-based configuration (Fig. 17), similar Q factors were obtained after 7100 km. Hence, OPC enabled a distance increase of 44%. Using CW tones, an average OSNR of 11.4 dB was measured after 10 200-km transmission. This OSNR is lower than initially reported in [29] due to more accurate measurements of the OSNR. The OSNR for the DCF-based configuration after 7100-km transmission is 12.1 dB. Given the average Q factor after transmission (10 and 9.7 dB for the OPC-aided and the DCF-aided setup, respectively), this coincides with an OSNR penalty compared to back-to-back of 1.1 dB for the OPC-based configuration and 2.0 dB for the DCF-based configuration.

The variance in Q factor per channel for the OPC-aided transmission after the 10 200-km transmission (Fig. 22) is larger than in the DCF-aided transmission after 7100-km transmission (Fig. 17). This results partly from the fact that the Q factors of the OPC-aided transmission are measured after 36 circulations through the loop instead of the 25 circulations in the DCF case. Also, in the OPC configuration, the 22 measured channels propagated the first half of the link in the upper part of the C band (1546.1 to 1554.5 nm) and, after OPC, the second half of the link in the lower part of the C band (1532.3 to 1540.6 nm), which complicates the spectral flattening with a DGE in the OPC-based configuration.

IV. Conclusion

We showed in a proof-of-principle experiment that an OPC can be employed to compensate for SPM-induced nonlinear phase noise in phase-shift-keyed transmission systems. In both the simulation and the experiment, a Q-factor improvement of over 4 dB is obtained for a low transmitted OSNR when OPC is employed. Also, the performance of DWDM 21.4-Gb/s DQPSK is compared for DCF- and OPC-aided transmission systems over a long haul distance. We show that the performance of the DCF-based scheme is impaired by SPM-induced nonlinear impairments such as nonlinear phase noise, whereas the performance of the OPC-aided transmission is virtually unaffected. This indicates that nonlinear phase noise is effectively compensated in a midlink OPC-based configuration.

References

[1] M. Daikoku, N. Yoshikane, and I. Morita, "Performance comparison of modulation formats for 40 Gb/s DWDM transmission systems," presented at the Optical Fiber Communication (OFC), Anaheim, CA, 2005, Paper OFN2.

[2] A. H. Gnauck and P. J. Winzer, "Optical phase-shift-keyed transmission," *J. Lightw. Technol.*, vol. 23, no. 1, pp. 115–130, Jan. 2005.

[3] C. Wree, J. Leibrich, and W. Rosenkranz, "RZ-DQPSK format with high spectral efficiency and high robustness towards fiber nonlinearities," presented at the Eur. Conf. Optical Communication (ECOC), Copenhagen, Denmark, 2002, Paper 9.6.6.

[4] A. H. Gnauck, P. J. Winzer, S. Chandrasekhar, and C. Dorrer, "Spectrally efficient (0.8 b/s/Hz) 1-Tb/s (25 × 42.7 Gb/s) RZ-DQPSK transmission over 28 100-km SSMF spans with 7 optical add/drops," presented at the Eur. Conf. Optical Communication (ECOC), Stockholm, Sweden, 2004, Paper Th4.4.1.

[5] J. P. Gordon and L. F. Mollenauer, "Phase noise in photonic communications systems using linear amplifiers," *Opt. Lett.*, vol. 15, no. 23, pp. 1351–1353, Dec. 1990.

[6] H. Kim and A. H. Gnauck, "Experimental investigation of the performance limitation of DPSK systems due to nonlinear phase noise," *IEEE Photon. Technol. Lett.*, vol. 15, no. 2, pp. 320–322, Feb. 2003.

[7] J. Hansryd, J. Howe, and C. Xu, "Experimental demonstration of nonlinear phase jitter compensation in DPSK modulated fiber links," *IEEE Photon. Technol. Lett.*, vol. 17, no. 1, pp. 232–235, Jan. 2005.

[8] P. S. Devgan, M. Shin, V. S. Grigoryan, J. Lasri, and P. Kumar, "SOA-based regenerative amplification of phase noise degraded DPSK signals," presented at the Optical Fiber Communication (OFC), Anaheim, CA, 2005, Paper PDP34.

[9] S. L. Jansen, D. van den Borne, C. Monsalve, S. Spälter, P. M. Krummrich, G. D. Khoe, and H. de Waardt, "Reduction of nonlinear phase noise by mid-link spectral inversion in a DPSK based transmission system," presented at the Optical Fiber Communication (OFC), Anaheim, CA, 2005, Paper OThO5.

[10] ——, "Reduction of Gordon–Mollenauer phase noise by mid-link spectral inversion," *IEEE Photon. Technol. Lett.*, vol. 17, no. 4, pp. 923–925, Apr. 2005.

[11] A. Yariv, D. Fekete, and D. M. Pepper, "Compensation for channel dispersion by nonlinear optical phase conjugation," *Opt. Lett.*, vol. 4, no. 2, pp. 52–54, Feb. 1979.

[12] S. Y. Set, R. Girardi, B. E. Riccardi, B. E. Olsson, M. Puleo, M. Ibsen, R. I. Laming, P. A. Andrekson, F. Cisternino, and H. Geiger, "40 Gb/s field transmission over standard fibre using midspan spectral inversion for dispersion compensation," *Electron. Lett.*, vol. 35, no. 7, pp. 581–582, Apr. 1999.

[13] D. D. Marcenac, D. Nesset, A. E. Kelly, M. Brierley, A. D. Ellis, D. G. Moodie, and C. W. Ford, "40 Gb/s transmission over 406 km of NDSF using mid-span spectral inversion by four-wave-mixing in a 2 mm long semiconductor optical amplifier," *Electron. Lett.*, vol. 33, no. 10, pp. 879–880, May 1997.

[14] U. Feiste, R. Ludwig, E. Dietrich, S. Diez, H. J. Ehrke, D. Razic, and H. G. Weber, "40 Gb/s transmission over 434 km standard-fiber using polarisation independent mid-span spectral inversion," *Electron. Lett.*, vol. 34, no. 21, pp. 2044–2045, Oct. 1998.

[15] S. L. Jansen, S. Spälter, G.-D. Khoe, H. de Waardt, H. E. Escobar, L. Marshall, and M. Sher, "16 $\times$ 40 Gb/s over 800 km of SSMF using mid-link spectral inversion," *IEEE Photon. Technol. Lett.*, vol. 16, no. 7, pp. 1763–1765, Jul. 2004.

[16] S. Watanabe and M. Shirasaki, "Exact compensation for both chromatic dispersion and Kerr effect in a transmission fiber using optical phase conjugation," *J. Lightw. Technol.*, vol. 14, no. 3, pp. 243–248, Mar. 1996.

[17] I. Brener, B. Mikkelsen, K. Rottwitt, W. Burkett, G. Raybon, J. B. Stark, K. Parameswaren, M. H. Chou, M. M. Fejer, E. E. Chaban, R. Harel, D. L. Philen, and S. Kosinski, "Cancellation of all Kerr nonlinearities in long fiber spans using a $LiNbO_3$ phase conjugator and Raman amplification," in *Proc. Optical Fiber Communication (OFC)*, Baltimore, MD, 2000, pp. 266–268, Paper PD33.

[18] A. Chowdhury, G. Raybon, R.-J. Essiambre, J. Sinsky, A. Adamiecki, J. Leuthold, C. R. Doerr, and S. Chandrasekhar, "Compensation of intrachannel nonlinearities in 40 Gb/s pseudo linear systems using optical phase conjugation," presented at the Optical Fiber Communication (OFC), Los Angeles, CA, 2004, Paper PDP 32.

[19] A. Chowdhury, G. Raybon, R.-J. Essiambre, and C. R. Doerr, "Optical phase conjugation in a WDM CSRZ pseudo-linear 40 Gb/s system for 4800 km transmission," presented at the Eur. Conf. Optical Communication (ECOC), Stockholm, Sweden, 2004, Paper Th4.5.6.

[20] J. Yamawaku, H. Takara, T. Ohara, K. Sato, A. Takada, T. Morioka, O. Tadanaga, H. Miyazawa, and M. Asobe, "Simultaneous 25 GHz-spaced DWDM wavelength conversion of 1.03 Tb/s (103 $\times$ 10 Gb/s) signals in PPLN waveguide," *Electron. Lett.*, vol. 39, no. 15, pp. 1144–1145, Jul. 2003.

[21] S. L. Jansen, G.-D. Khoe, H. de Waardt, S. Spälter, C.-J. Weiske, A. Schöpflin, S. J. Field, H. E. Escobar, and M. H. Sher, "Mixed data rate and format transmission (40 Gb/s NRZ, 40 Gb/s duobinary, 10 Gb/s NRZ) using mid-link spectral inversion," *Opt. Lett.*, vol. 29, no. 20, pp. 2348–2350, Oct. 2004.

[22] A. Chowdhury and R.-J. Essiambre, "Optical phase conjugation and pseudolinear transmission," *Opt. Lett.*, vol. 29, no. 10, pp. 1105–1107, May 2004.

[23] S. L. Jansen, S. Calabró, B. Spinnler, D. van den Borne, P. M. Krummrich, G. D. Khoe, and H. de Waardt, "Nonlinear phase noise reduction in DPSK transmission by optical phase conjugation," in *Proc Optoelectronics and Communications Conf. (OECC)*, Seoul, Korea, 2005, pp. 174–175, Paper 6B1-3.

[24] M. C. Jeruchim, P. Balaban, and K. S. Shanmugan, *Simulation of Communication Systems*. New York: Plenum, 1992.

[25] C. J. McKinstrie, S. Radic, and C. Xie, "Reduction of soliton phase jitter by in-line phase conjugation," *Opt. Lett.*, vol. 28, no. 17, pp. 1519–1521, Sep. 2004.

[26] H. Griesser and J. P. Elbers, "Influence of cross-phase modulation induced nonlinear phase noise on DQPSK signals from neighbouring OOK channels," presented at the Eur. Conf. Optical Communication (ECOC), Glasgow, U.K., 2005, Paper Tu1.2.2.

[27] T. Mizuochi, K. Ishida, T. Kobayashi, J. Abe, K. Kinjo, K. Motoshima, and K. Kasahara, "A comparative study of DPSK and OOK WDM transmission over transoceanic distances and their performance degradations due to nonlinear phase noise," *J. Lightw. Technol.*, vol. 21, no. 9, pp. 1933–1943, Sep. 2003.

[28] C. Rasmussen, S. Dey, F. Liu, J. Bennike, B. Mikkelsen, P. Mamyshev, M. Kimmitt, K. Springer, D. Gapontsev, and V. Ivshin, "Transmission of 40 $\times$ 42.7 Gb/s over 5200 km UltraWave fiber with terrestrial 100 km spans using turn-key ETDM transmitter and receiver," presented at the Eur. Conf. Optical Communication (ECOC), Copenhagen, Denmark, 2002, Paper PD4.4.

[29] S. L. Jansen, D. van den Borne, C. Climent, M. Serbay, C.-J. Weiske, H. Suche, P. M. Krummrich, S. Spälter, S. Calabró, N. Hecker-Denschlag, P. Leisching, W. Rosenkranz, W. Sohler, G. D. Khoe, T. Koonen, and H. de Waardt, "10 200 km 22 $\times$ 2 $\times$ 10 Gb/s RZ-DQPSK dense WDM transmission without inline dispersion compensation through optical phase conjugation," presented at the Optical Fiber Communication (OFC), Anaheim, CA, 2005, Paper PDP28.

[30] C. Q. Xu, H. Okayama, and M. Kawahara, "1.5 μm band efficient broadband wavelength conversion by difference frequency generation in a periodically domain-inverted $LiNbO_3$ channel waveguide," *Appl. Phys. Lett.*, vol. 63, no. 26, pp. 3559–3561, Dec. 1993.

[31] M. H. Chou, J. Hauden, M. A. Arbore, and M. M. Fejer, "1.5-μm-band wavelength conversion based on difference-frequency generation in $LiNbO_3$ waveguides with integrated coupling structures," *Opt. Lett.*, vol. 23, no. 13, pp. 1004–1006, Jul. 1998.

[32] D. Caccioli, A. Paoletti, A. Schiffini, A. Galtarossa, P. Griggio, G. Lorenzetto, P. Minzioni, S. Cascelli, M. Guglielmucci, L. Lattanzi, F. Matera, G. M. Tosi Beleffi, V. Quiring, W. Sohler, H. Suche, S. Vehovc, and M. Vidmar, "Field demonstration of in-line all-optical wavelength conversion in a WDM dispersion managed 40-Gb/s link," *IEEE J. Sel. Topics Quantum Electron.*, vol. 10, no. 2, pp. 356–362, Mar./Apr. 2004.

S. L. Jansen (S'02) was born in Maartensdijk, The Netherlands, in 1978. He received the M.Sc. degree in 2001 and is currently pursuing the Ph.D. degree in collaboration with the Siemens AG, Munich, Germany, from the University of Technology, Eindhoven, The Netherlands, all in electrical engineering. He conducted his Master's thesis at Siemens AG.

He worked at Siemens AG as part of the high-speed research team for the European funded Information Society Technologies (IST) project Ultra fast Switching in High-Speed Optical Time-Division Multiplexing (OTDM) Networks (FASHION) on ultrafast optical switching in semiconductor optical amplifiers. His main research interests include optical regeneration, optical phase conjugation (OPC), and alternative modulation formats. He is the author or coauthor of more than 30 refereed papers and conference contributions.

Mr. Jansen was awarded the IEEE Lasers and Electro-Optics Society (LEOS) Graduate Student Fellowship in 2005.

D. van den Borne (S'04) was born in Bladel, The Netherlands, on October 7, 1979. He received the M.Sc. degree (*cum laude*) in 2004 and is currently pursuing the Ph.D. degree in collaboration with Siemens AG, Munich, Germany, working on advanced modulation formats for optical communication links, from Eindhoven University of Technology, The Netherlands, all in electric engineering. He performed his Master's thesis work in collaboration with Siemens AG on polarization mode dispersion (PMD)-related transmission penalties in polarization-multiplexed transmission.

He previously worked at Fuijtsu laboratories Ltd., Kawasaki, Japan, on supercontinuum generation and pulse compression.

B. Spinnler was born in Erlangen, Germany, in 1968. He received the Dipl.Ing. degree in communications engineering in 1994 and the Dr.Ing. degree in 1997 with a thesis on noncoherent detection of continuous phase modulation, all from the University of Erlangen-Nürnberg, Germany.

From 1994 to 1997, he was a Research Scientist at the Institut für Integrierte Schaltungen, Fraunhofer Gesellschaft, and at the Lehrstuhl für Nachrichtentechnik, the University of Erlangen-Nürnberg. From 1997, he worked on low-complexity modem design of wireless radio relay systems at Siemens AG–Information and Communication Networks. In 2002, he joined the optical networks group of Siemens Corporate Technology where he worked on robust and tolerant design of optical communications systems. His current interests focus on advanced modulation, forward error correction (FEC), and equalization.

S. Calabrò received the Ing. degree ("Laurea") and the Doctoral degree in digital communications in 1995 and 1999, respectively, all from the University of Palermo, Italy.

Since 1999, he has been with Siemens AG, Munich, Germany. From 1999 to 2001, he worked at the development of modems for wireless communications. Since 2001, he has been working as a Research Engineer in the field of optical communications.

H. Suche received the Diplom-Physiker and the Dr.Rer.Nat. degrees from the University of Dortmund, Germany, in 1978 and 1981, respectively, all in physics.

In 1981, he joined the Fraunhofer Institut für Physikalische Meßtechnik, Freiburg, Germany, as a Research Member in the Department of Fibre Optic Sensors. Since 1982, he has been with the University of Paderborn, Germany. His research interests include nonlinear integrated optics, laser physics, and material science. He is the author or coauthor of about 100 journals and conference contributions and of several book chapters.

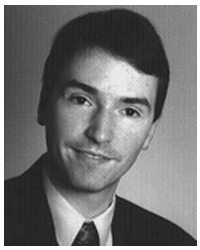

P. M. Krummrich (M'05) received the Dipl.Ing. and Dr. Ing. degrees in 1992 and 1995, respectively, from the Technical University of Braunschweig, Germany, all in electrical engineering.

He worked at the Technical University of Braunschweig on the field of wavelength tuning of laser diodes using external cavities and praseodymium-doped fiber amplifiers. In 1995, he joined Siemens AG, Munich, Germany, where his research interest focused on distributed erbium-doped fiber amplifiers. He is currently working on technologies for the next generation of ultrahigh capacity dense wavelength division multiplexing (DWDM) transmission systems with focus on technologies enabling to enhance system reach such as Raman amplification, advanced modulation formats, adaptive equalizers, and polarization mode dispersion (PMD) compensation.

W. Sohler, photograph and biography not available at the time of publication.

G.-D. Khoe (S'71–M'71–SM'85–F'91) was born in Magelang, Indonesia, on July 22, 1946. He received the electrical engineering degree (*cum laude*) from the Eindhoven University of Technology, Eindhoven, The Netherlands, in 1971.

He began his research career at the Dutch Foundation for Fundamental Research on Matter (FOM) Laboratory on Plasma Physics, Rijnhuizen, The Netherlands. In 1973, he moved to Philips Research Laboratories to research on the area of optical fiber communication systems. In 1983, he was appointed as a Part Time Professor at Eindhoven University of Technology, where he became a Full Professor in 1994 and is currently the Chairman of the Department of Telecommunication Technology and Electromagnetics (TTE). Most of his works have been devoted to single-mode fiber systems and components. Currently, his research programs are centered on ultrafast all-optical signal processing, high-capacity transport systems, and systems in the environment of the users. He is the author or coauthor of more than 100 papers, invited papers, and chapters in books. He is the holder of more than 40 U.S. patents.

Dr. Khoe was the General Co-Chair of European Conference on Optical Communication (ECOC) 2001 and was a Founder of the Lasers and Electro-Optics Society (LEOS) Benelux Chapter. He received the micro-optics conference/graded-index optical (MOC/GRIN) award in 1997. In 2003, he was appointed as President of LEOS.

H. de Waardt was born in Voorburg, The Netherlands, in December, 1953. He received the M.Sc.E.E. and Ph.D. degrees from Delft University of Technology, The Netherlands, in 1980 and 1995, respectively.

In 1981, he started his professional career in the Physics Department at PTT Research, Leidschendam, The Netherlands, where he worked on the performance issues of optoelectronic devices. In 1989, he moved to the Transmission Department and became involved in wavelength division multiplexing (WDM) high-bit-rate optical transmission. In 1995, he was appointed as an Associate Professor at the Eindhoven University of Technology (TU/e), Eindhoven, The Netherlands, in the area of high-capacity trunk transmission. He coordinated the participation of TU/e in Advanced Communication Technologies and Systems (ACTS) Upgrade, ACTS Broadband Lightware Sources and Systems (BLISS), ACTS Advanced Photonic Experimetal X-connect (APEX), and Information Society Technologies Ultrafast Switching in High-Speed Optical Time-Division Multiplexing (OTDM) Networks (IST FASHION). Presently, he is the Project Leader of the National Research Initiative Freeband Broadband Photonics (2004–2008). His current interests include high-capacity optical transmission and networking, integrated optics, and semiconductor optical amplifiers. He is the author or coauthor of more than 100 conference and journal papers.

Dr. de Waardt is member of the IEEE Laser and Electro-Optics Society (LEOS).